Information Gain for the Pulse Width Modulation of a Square Waveform by Continued Signal Tracking through a Second Pulse

by

Frank Lad

Department of Mathematics and Statistics

University of Canterbury, Christchurch, New Zealand

and

G.R. Dunlop

Department of Mechanical Engineering

University of Canterbury, Christchurch, New Zealand

No. 136 February, 1996

Abstract – We continue the analysis of information about the pulse width modulation of a square wave signal to derive the posterior density of the pwm ratio given digital counts of on and off components of two pulses when the second is an exact replica of the first. A propagation equation for the phase shift disturbance allows that sequential counts, which can occur in only seven distinct structures, rule out various portions of the unit cube as containing the unknown disturbance fractions. Again, the analysis uses only elementary arguments in the calculus of many variables, but the structure of the setup becomes extremely complicated. We provide complete analysis in the simplest of the seven cases, and display the resulting posterior distribution and density properties under the condition of the two-pulse counts being $M_1 = 100$, $N_1 = 1000$, $M_2 = 101$, and $N_2 = 1001$. Algebraic and graphical detail is produced using MAPLE software.

Keywords – Repeated Signals, Propagation Equations.

Information Gain for the Pulse Width Modulation of a Square Waveform by Continued Signal Tracking through a Second Pulse

Frank Lad and G. R. Dunlop

Dept. of Mathematics and Statistics Dept. of Mechanical Engineering

University of Canterbury
Christchurch, New Zealand

7 February, 1996

1. Introduction

For the context of precise measurement, we have derived (Lad and Dunlop, 1996) the posterior density and related characteristics of uncertainty about the pulse width modulation of a square wave conditioned on digital counts of its on and off components via the vibrations of a pulsating crystal. An important signature of the amount of information contained in the data is the size of N_1, the number of vibration counts recorded during the complete wave (both on and off components.) As a telling feature of this count, the posterior density is positive only over the interval $[(M_1 - 1)/N_1, (M_1 + 1)/N_1]$, which obviously contracts as N_1 increases. Thus, a crude but expensive way to increase the precision of our understanding the signal from a square wave is to use a counting crystal that vibrates faster, yielding more counts per square wave. However, even with all the money in the world there is a limit to the speed of crystal vibrations that can be achieved in a counting device.

The next matter for investigation is the gain in information regarding the pwm that can be achieved more cheaply by continuing the registered pulse count statistics through a second square wave of an on-off signal, ... and even through a third, fourth, or more waves. Of course the longer is the duration of registered counts, the greater becomes the opportunity for the temperature (or whatever characteristic producing the square wave) of the system being monitored to change. These issues can be addressed precisely.

The present report derives the posterior density and related characteristics of uncertainty regarding a pwm ratio conditioned on crystal vibration counts of two successive square wave signals, *under the supposition that* the second signalling wave is an exact replica of the first. This is an important next step in developing a full understanding of the information transfer from a signal process. Once it is completed, issues related to

understanding a changing signal and garnering information about its rate of change can be addressed. As we shall see, our supposition does *not* imply that the vibration counts M_2 and N_2 registered during the second wave are identical to the counts M_1 and N_1 registered during the first wave. But if the *waves* are identical, there is a precise limitation to the form of the differences between successive counts. Moreover, each particular possible form of the count sequence to be registered emits a different amount of information regarding the pwm ratio.

The details of the information transfer from a sequence of repeated wave signals become extremely complicated, although their characterisation is still completely tractable. We shall exhibit complete details of the derivation of the posterior distribution in only one of its possible conditioning measurement scenarios. A report on the complete programming system for all scenarios will appear as technical monograph. Again, all relevant programs, conducted in MAPLE, are available from the authors.

All definitions and notations of our preceding report regarding the first signal wave are presumed, and indeed their understanding is required for continuing with the present report. In Section 2 we shall formulate the propagation equation for the phase-shift epsilon for a second signalling wave, to be denoted ϵ_1, as a function of the values of ϵ_0, ϵ_τ, and ϵ_T appropriate to the first wave. Section 3 then derives the relevance of the relative positioning of ϵ_1 within the ordering of ϵ_0, ϵ_τ, and ϵ_T to the measurement sequence M_1, N_1, M_2, and N_2. Rather than merely six partitioning regions of the unit-cube, the posterior analysis of *two* signal pulses requires a designation of 16 partitioning regions that need distinct analysis. In Section 4 we exhibit the method of analysing just two of these regions, which are relevant to the simplest of (what are found to be) the seven possible data-conditioning-scenarios. Section 5 exhibits the resulting posterior density in the specific instance of observing $M_1 = 100$, $N_1 = 1000$, $M_2 = 101$, and $N_2 = 1001$, and compares it with the posterior conditioned on a single wave count of $M_1 = 201$ and $N_1 = 2001$. Concluding remarks and an outline of further directions for work constitute Section 6.

2. Propagation Equation for Sequential Values of Phase-shift Epsilons

For the pulse count M_2 registered during the second square wave, the relation of the crystal vibration counts to the signalling wave has exactly the same *structure* as for the first wave. The only difference is that the size of "ϵ_0" for the second wave, the proportion of the first "counted" crystal stroke interval in the current-on state that the electronic system actually rests in the current-on state, is emended to ϵ_1, a function only of ϵ_0 and ϵ_T specified by

$$\epsilon_1 = 1 - \epsilon_T + \epsilon_0 - (1 - \epsilon_T + \epsilon_0 \geq 1)$$
$$= \epsilon_0 - \epsilon_T + (\epsilon_0 < \epsilon_T). \qquad (1)$$

This function can be understood by examining Fig. 1 (which develops Fig. 4 of our preceding report), and noticing the determination of ϵ_1 in each of the three cases of $\epsilon_0 < \epsilon_\tau$, $\epsilon_\tau \leq \epsilon_0 < \epsilon_T$, and $\epsilon_T \leq \epsilon_0$. We shall discuss particulars of this examination below the printed Figure. By definition, the size of ϵ_1 equals the proportion of a counting interval Δ that remains after time $t_0 + T$ before the first click is registered in the current-on state for the second wave. The idea motivating equation (1) in its first form, is that in determining ϵ_1, $1 - \epsilon_T$ is augmented by ϵ_0 unless this sum equals or exceeds 1, in which case this sum would be reduced by 1. The second line of equation (1) presents a simpler, but equivalent algebraic formulation.

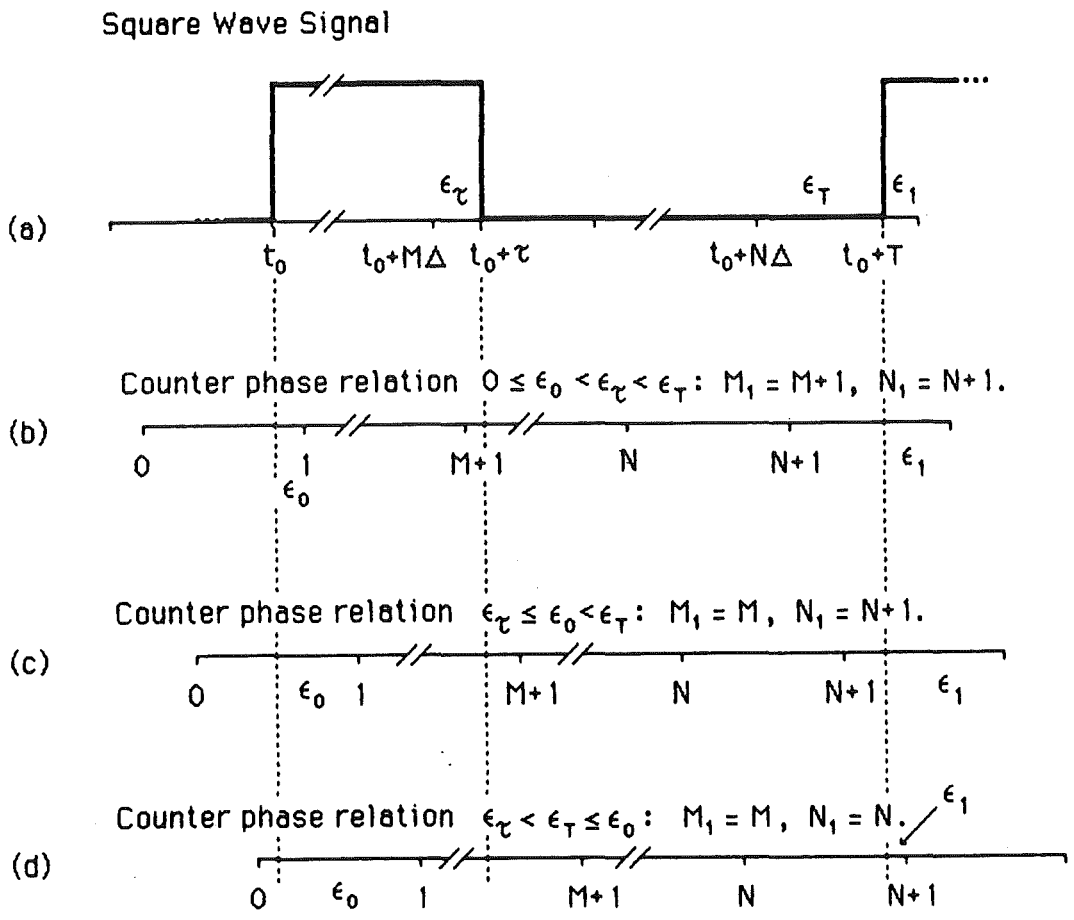

Figure 1. At the right end of each shifted phase relation (lines a - d) the value of ϵ_1 is identified as the proportion of a crystal count interval that the first "counted" stroke in the second wave corresponds to an "on" component of the second wave. In each case, the value of ϵ_1 is described algebraically according to equation (1) by $\epsilon_0 - \epsilon_T + (\epsilon_0 < \epsilon_T)$.

In Fig. 1a, the value of ϵ_0 is equal to $)1 \geq \epsilon_T$, and thus the value of ϵ_1 derived from equation (1) equals $1 - \epsilon_T$, which is easily seen in the Figure. In Fig. 1b, ϵ_0 is both small (smaller even than ϵ_τ) and less than ϵ_T; equation (1) thus resolves to $\epsilon_1 = 1 - \epsilon_T + \epsilon_0$, which can also be gleaned from the Figure. In Fig. 1c, ϵ_0 is greater than in 1b (greater now even than ϵ_τ), but still smaller than ϵ_T. Thus, ϵ_1 shown in 1c exceeds ϵ_1 in 1b by the difference in the sizes of ϵ_0 for the two cases. Finally, in Fig. 1d the value of ϵ_0 is so great (larger even than ϵ_T) that when added to $1 - \epsilon_T$, the sum exceeds 1, and thus must be diminished by 1 as specified by the negative of $(\epsilon_0 > \epsilon_T)$ in equation (1). Although Fig. 1 is constructed to represent the situation when $\epsilon_\tau < \epsilon_T$, the functional representation of ϵ_1 by equation (1) covers the alternative situation that $\epsilon_T \leq \epsilon_\tau$ as well. In either case, an important feature of this result is that the size of ϵ_τ is irrelevant to determining the value of ϵ_1.

Since the structure of phase-shift epsilon propogation for subsequent waves would remain the same as long as the square wave signals continue to replicate, equation (1) generalises to the recursive equation

$$\epsilon_i = \epsilon_{i-1} - \epsilon_T + (\epsilon_{i-1} < \epsilon_T) \qquad (2)$$

to represent the measurement structure of an i^{th} exactly repeating square wave. Our study of the information content of a measurement sequence $\{M_1, N_1, M_2, N_2, M_3, N_3, \ldots\}$ regarding the pwm τ/T now proceeds with the asserted uniform distribution of $(\epsilon_0, \epsilon_\tau, \epsilon_T)$ over the unit-cube, conditionally independent given the values of M_1 and N_1. (We shall extend this "prior" assertion mildly when appropriate.) It is worth mentioning that based on this assertion, the associated value of ϵ_1 and subsequent values of ϵ_i are *not* conditionally independent of $(\epsilon_0, \epsilon_\tau, \epsilon_T)$. The analysis of the correlation and joint distribution structure among successive values of the phase-shift ϵ_i's is tractable and intriguing as an excercise, but its substantive content relevant to our understanding of the pwm is derived more easily by direct methods, to which we now turn.

In measuring the second wave signal then, the determination of M_2 and N_2, the number of registered pulse counts in the signal-on state, and the total number of registered counts during the complete wave respectively, are according to the equations

$$M_2 = M + 1 - (\epsilon_1 \geq \epsilon_\tau) \quad \text{and} \quad N_2 = N + 1 - (\epsilon_1 \geq \epsilon_T);$$

$$\text{and generally,} \quad M_i = M + 1 - (\epsilon_{i-1} \geq \epsilon_\tau) \quad \text{and} \quad N_i = N + 1 - (\epsilon_{i-1} \geq \epsilon_T) \qquad (3)$$

for the i^{th} square wave measurement, where the values of ϵ_i are generated recursively by equation (2). As a result of equation (3), after vibration counts through two pulses of the square wave, we have two equivalent representations for the values of τ and T:

$$\tau = M_1 - 1 + (\epsilon_0 \geq \epsilon_\tau) + \epsilon_\tau = M_2 - 1 + (\epsilon_1 \geq \epsilon_\tau) + \epsilon_\tau \text{ , and}$$
$$T = N_1 - 1 + (\epsilon_0 \geq \epsilon_T) + \epsilon_T = N_2 - 1 + (\epsilon_1 \geq \epsilon_T) + \epsilon_T .$$

Thus, the pwm ratio τ/T can be represented via the two pulse measurements by summing these two numerator and denominator representations to yield

$$\tau/T = \frac{M_1 + M_2 - 2 + (\epsilon_0 \geq \epsilon_\tau) + (\epsilon_1 \geq \epsilon_\tau) + 2\epsilon_\tau}{N_1 + N_2 - 2 + (\epsilon_0 \geq \epsilon_T) + (\epsilon_1 \geq \epsilon_T) + 2\epsilon_T} \quad . \tag{4}$$

As in our analysis of vibration counts from a single square wave, the awkward feature of equation (4) relevant to deriving the posterior density of the pwm conditioned on M_1, M_2, N_1, and N_2 derives from the quantum jumps in the numerator and denominator (now four possibilities) when the values of ϵ_0 and ϵ_1 cross the boundary values of ϵ_τ and ϵ_T. The resolution of this difficulty can again be achieved by conditioning our analysis on subregions of the unit-cube in which the Heaviside events $(\epsilon_0 \geq \epsilon_\tau)$, $(\epsilon_1 \geq \epsilon_\tau)$, $(\epsilon_0 \geq \epsilon_T)$, and $(\epsilon_1 \geq \epsilon_T)$ are unequivocal. The complexity of this partitioning programme expands almost geometrically upon the analysis for a single wave. We now turn to its detail.

3. Partitioning the Unit-Cube into Unequivocal Quantum States

Remember that when pursuing the similar but relatively simple partitioning of the cube for analysing the counts for a single wave, we constructed the partition from the six possible orderings of ϵ_0, ϵ_τ, and ϵ_T. The region we designated as 1A, for example, involved $\epsilon_0 < \epsilon_\tau < \epsilon_T$. When analysing counts from the second wave pulse, an unequivocal resolution of the event components of equation (4) is achieved only if the size of $\epsilon_1 = \epsilon_0 - \epsilon_T + (\epsilon_0 < \epsilon_T)$ is determined within this inequality ordering. On first consideration it appears there are four possibilities within Region 1A, beginning with $\epsilon_1 < \epsilon_0 < \epsilon_\tau < \epsilon_T$, and successively advancing the size of ϵ_1 through the ordering. On further investigation, we find that the first of these "possibilities" is actually impossible, since under the presumption that $\epsilon_0 < \epsilon_\tau < \epsilon_T$, the algebraic representation of ϵ_1 resolves to

$$\epsilon_1 = \epsilon_0 - \epsilon_T + (\epsilon_0 < \epsilon_T) = \epsilon_0 + 1 - \epsilon_T ,$$

which is surely at least as large as ϵ_0.

In specifying the constituents of the partition of the unit-cube required for an unequivocal evaluation of the event-components of equation (4), we begin by defining three constituent regions we shall label 1A1, 1A2, and 1A3 as

Region 1A1: $\epsilon_0 \leq \epsilon_1 < \epsilon_\tau < \epsilon_T \approx \epsilon_0 < \epsilon_\tau + \epsilon_T - 1 < \epsilon_T$;

1A2: $\epsilon_0 < \epsilon_\tau \leq \epsilon_1 < \epsilon_T \approx \epsilon_\tau + \epsilon_T - 1 \leq \epsilon_0 < \epsilon_\tau$ *and* $\epsilon_0 < 2\epsilon_T - 1$; and

1A3: $\epsilon_0 < \epsilon_\tau < \epsilon_T \leq \epsilon_1 \approx 2\epsilon_T - 1 \leq \epsilon_0 < \epsilon_\tau < \epsilon_T$.

The "equivalent" characterization of each region on the right-hand side of these specifications is derived from replacing ϵ_1 in the ordering representation on the left-hand side by its equivalent expression from evaluating equation (1) as $\epsilon_1 = \epsilon_0 + 1 - \epsilon_T$, since $\epsilon_0 < \epsilon_T$ everywhere within Region 1A.

A similar subpartitioning of the constituent Regions 1B, 1C, 2A, 2B, and 2C of the cube is achievable only by careful attention, since the detail is different in every case. Table 1 summarises the results. (It appears after the references.) The purpose of defining the three subregions of the partitioning Region 1A is that the events defining τ/T in equation (4) are unequivocal therein:

$$\begin{aligned} \tau/T &= (M_1 + M_2 - 2 + 2\epsilon_\tau) / (N_1 + N_2 - 2 + 2\epsilon_T) \quad \text{when } (\epsilon_0, \epsilon_\tau, \epsilon_T) \blacksquare \text{ 1A1,} \\ &= (M_1 + M_2 - 1 + 2\epsilon_\tau) / (N_1 + N_2 - 2 + 2\epsilon_T) \quad \text{when } (\epsilon_0, \epsilon_\tau, \epsilon_T) \blacksquare \text{ 1A2, and} \\ &= (M_1 + M_2 - 1 + 2\epsilon_\tau) / (N_1 + N_2 - 1 + 2\epsilon_T) \quad \text{when } (\epsilon_0, \epsilon_\tau, \epsilon_T) \blacksquare \text{ 1A3.} \end{aligned}$$

Table 1 also summarises the characterisation of the pwm ratio τ/T within the sixteen partitioning regions of the unit-cube, derived by a similar subdivision of the six regions that partitioned the cube for the analysis of a single signal pulse. Finally, it identifies the values of M_1, N_1, M_2, and N_2 relative to M and N within each region.

The next step in the analysis is to determine the posterior density of τ/T conditional on M_1, N_1, M_2, and N_2, *and* conditional on the restriction of $(\epsilon_0, \epsilon_\tau, \epsilon_T)$ lying within each distinct region. To achieve this programme, we shall begin by deriving the probability of the epsilon vector lying within each region, and subsequently the joint density function for $(\epsilon_\tau, \epsilon_T)$ conditional on the subregion. Eventually, we shall determine the marginal posterior densities of τ/T conditional on $(\epsilon_0, \epsilon_\tau, \epsilon_T)$ lying within each region, and then appropriately accumulate them over all regions according to the law of total probability.

4. A Complete Posterior Analysis when $M_1 < M_2$ and $N_1 < N_2$

We shall complete the details of the posterior analysis for only the simplest scenario of the conditioning data that entails an instantiation of every complication involved in the analysis of all possible observation scenarios.

Recall that our posterior analysis for a single wave was based upon the prior assertion regarding the vector $(\epsilon_0, \epsilon_\tau, \epsilon_T)$ conditional on M_1 and N_1 as uniform over the unit-cube. For analysing the second wave we need to extend this assertion to the uniformity of this epsilon vector conditioned on any of the 16 regions identified in Table 1 *and* conditioned on a two-pulse count sequence that agrees with the said region. Examining Table 1 again, we can recognize that while the observation of M_1, N_1, M_2, and N_2 through the second pulse cannot identify the partitioning region in which the vector $(\epsilon_0, \epsilon_\tau, \epsilon_T)$ lies, it does reduce the possibilities to a greater or lesser extent. Notice that each of M_1 and M_2 can equal only either M or (M+1), and each of N_1 and N_2 only N or (N+1); moreover, in any instance we do not know whether it is the value of M or (M+1), say, that we are observing. Thus, the vibration counts from two pulses distinguish themselves only on the basis of whether $M_1 < M_2$, $M_1 = M_2$, or $M_1 > M_2$, and whether $N_1 < N_2$, $N_1 = N_2$, or $N_1 > N_2$, amounting to 9 possibilities.

Table 2 identifies the various regions among the 16 defined in Table 1 that yield each of the 9 "possible" observation scenarios. The quotations are deserved because, in fact, two of the scenarios are found to be impossible! Examining Table 1 shows that whenever $M_1 < M_2$, either $N_1 < N_2$ or $N_1 = N_2$. In no region is it the case that $M_1 < M_2$ *and* $N_1 > N_2$. This fact is designated in Table 2, as is the impossibility of the reflective condition of $M_1 > M_2$ *and* $N_1 < N_2$. The other seven observation relations among the two-pulse counts are found to identify either one, two, or six regions that support them. An interesting distinction can be seen by comparing the observation relations $M_1 < M_2$ and $N_1 < N_2$, instantiated in regions 1C1 and 2C1, with the relations $M_1 = M_2$ and $N_1 < N_2$ which are instantiated in regions 1C2 and 2B1. In the case of the former relation, both supporting observation vectors are identical: $(M_1, N_1, M_2, N_2) = (M, N, M+1, N+1)$. When supporting the latter relation, the observation vector $(M_1, N_1, M_2, N_2) = (M, N, M, N+1)$ in Region 1C2, while in Region 2B1 the observation vector $(M_1, N_1, M_2, N_2) = (M+1, N, M+1, N+1)$, which is distinctly different ... *but unrecognizably so.* To repeat, when observing any vibration count M_i or N_i, we cannot know whether it is M or (M+1), or N or (N+1) that we are observing. This situation occurs with greater vengeance when $M_1 = M_2$ *and* $N_1 = N_2$, a relation that can occur in four possible ways over six regions, designated in Table 2.

To conclude our presentation here, we shall complete all details of the posterior analysis under the condition that $M_1 < M_2$ and $N_1 < N_2$ which occurs only when the epsilon vector lies within Regions 1C1 and 2C1. This turns out to be the simplest case for describing the method of analysis. The procedure is similar in the other conditioning scenarios, although the details are even more complicated.

4.1. The Prior Probability P(2C1) and Posterior Density $f(\epsilon_\tau, \epsilon_T | 2C1)$

In the context of precise measurement discussed in our previous report, the distribution of the epsilon vector $(\epsilon_0, \epsilon_\tau, \epsilon_T)$ is asserted as uniform over the unit-cube, $[0,1)^3$. As the analysis of Region 2C1 involves the minimum of maximal intrigue over all partitioning regions of the cube, we begin by deriving its prior probability via the integral of the uniform density over it.

To set up the integral, firstly realize that the Region 2C1, defined by $\epsilon_1 < \epsilon_T \leq \epsilon_\tau \leq \epsilon_0$, is defined equivalently by $\epsilon_0 - \epsilon_T < \epsilon_T \leq \epsilon_\tau \leq \epsilon_0$. This derives from resolving the propagation equation (1) within 2C1 to yield $\epsilon_1 = \epsilon_0 - \epsilon_T$, and making this replacement within the Region 2C1-defining inequality. We shall perform the integration over three variables firstly with respect to ϵ_T, secondly with respect to ϵ_τ, and finally with respect to ϵ_0. The bounds on ϵ_T are straightforward, from $\epsilon_0/2$ to ϵ_τ; the lower bound derives from the left-end inequality, $\epsilon_0 - \epsilon_T < \epsilon_T$, characteristic of the region. The bounds on ϵ_τ run, in turn, from $\epsilon_0/2$ to ϵ_0; the lower bound derives from the requirement that ϵ_τ must exceed ϵ_T which itself must exceed $\epsilon_0/2$. Finally, the integral over ϵ_0 runs over the entire interval from 0 to 1. To conclude then,

$$P[(\epsilon_0, \epsilon_\tau, \epsilon_T) \in 2C1] = \int_0^1 \int_{\epsilon_0/2}^{\epsilon_0} \int_{\epsilon_0/2}^{\epsilon_\tau} d\epsilon_T \, d\epsilon_\tau \, d\epsilon_0 = 1/24,$$

a resolution following from elementary methods of integration. It is worth mentioning that most of the partitioning region probabilities do not derive quite so simply. In most cases, the determination of the limits of integration is much trickier. For a more difficult exercise, the reader may wish to attempt the integral that specifies the probability of Region 1A1, for example, and even of Region 1A2, the most difficult and complicated of all. Full details for all regions will appear in our promised exhaustive technical monograph.

The next step in determining the posterior density of τ/T given M_1, N_1, M_2, and N_2 via equation (4) is to identify the joint density of ϵ_τ and ϵ_T conditioned within Region 2C1. This now requires the integration of the conditional density of $f(\epsilon_0, \epsilon_\tau, \epsilon_T | 2C1)$, which is constant at 24, merely with respect to the domain of ϵ_0. Although not difficult, this demands some care, for the boundary specifications for the integral differ depending on whether ϵ_T exceeds 1/2 or not. Let us state the result, and then discuss it with the aid of Fig. 2, which contains information relevant to subsequent analysis as well:

$$f(\epsilon_\tau, \epsilon_T \mid 2C1) = (\epsilon_T \le 1/2) \int_{\epsilon_\tau}^{2\epsilon_T} 24\, d\epsilon_0 + (\epsilon_T > 1/2) \int_{\epsilon_\tau}^{1} 24\, d\epsilon_0 ,$$

$$= (\epsilon_T \le 1/2)\ 24\,(2\epsilon_T - \epsilon_\tau) + (\epsilon_T > 1/2)\ 24\,(1 - \epsilon_\tau) , \quad (5)$$

where it is understood that $\epsilon_T \le \epsilon_\tau$. These integration boundaries are best understood by rewriting the Region-2C1-defining-inequality, $\epsilon_0 - \epsilon_T < \epsilon_T \le \epsilon_\tau \le \epsilon_0$, as $\epsilon_T \le \epsilon_\tau \le \epsilon_0 < 2\epsilon_T$. In this form it is evident that the upper boundary on ϵ_0 shifts from $2\epsilon_T$ to 1 when ϵ_T crosses the delimiting value of 1/2.

Figure 2 then displays on its right-hand-side the space of $(\epsilon_T, \epsilon_\tau)$ possibilities that are appropriate to the conditioning Region 2C1, projected through the ϵ_0 dimension. The delimiting lines $\epsilon_\tau = 2\epsilon_T$ and $\epsilon_\tau = \epsilon_T$ are clearly marked. The complete region is divided into two parts: subregion 2C11 corresponds to values of $\epsilon_T \le 1/2$, while subregion 2C12 corresponds to values of $\epsilon_T > 1/2$. Subdividing 2C1 into these two subregions is necessary to perform the margining integration to derive the conditional density $f(\tau/T \mid 2C1)$, since the algebraic form of the joint density is different in each case.

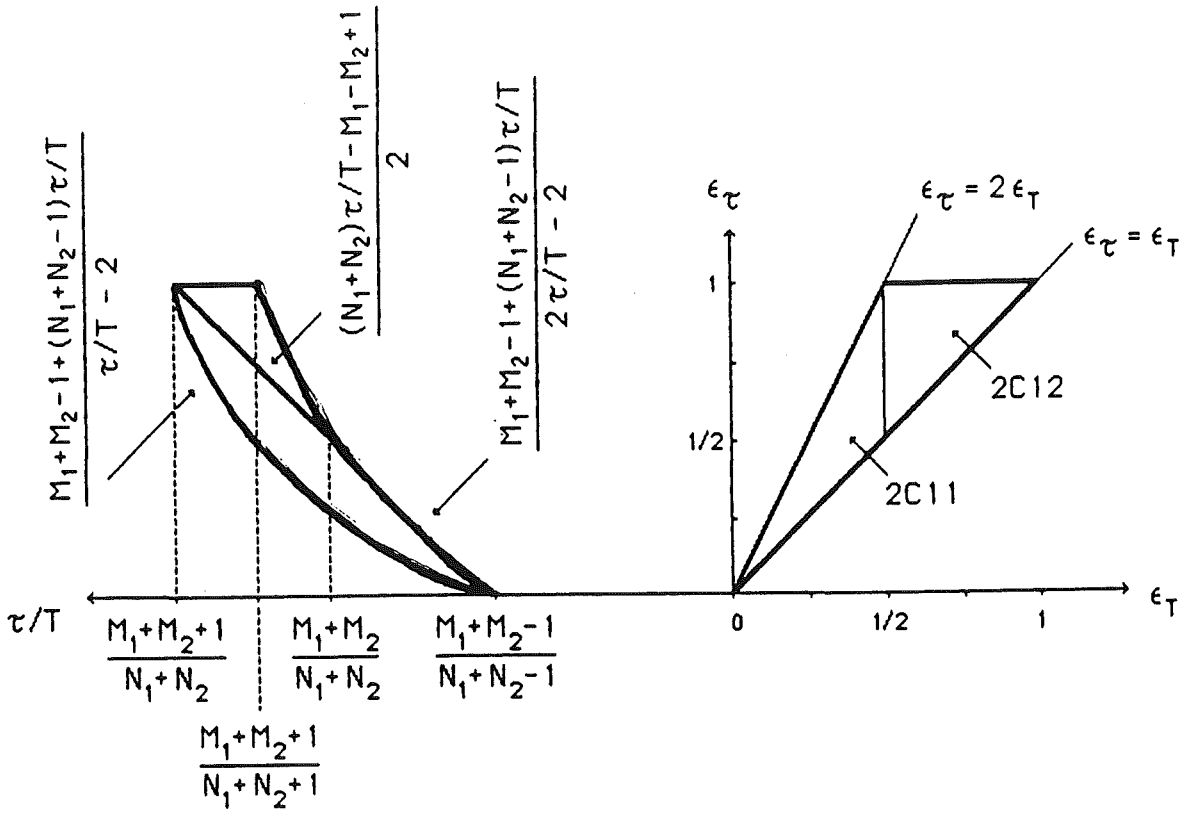

Figure 2. Region 2C1, projected into its $(\epsilon_T, \epsilon_\tau)$ dimensions at right, is transformed into a space of $(\tau/T, \epsilon_\tau)$ pairs at left.

4.2. Transforming the Posterior Density $f(\epsilon_\tau, \epsilon_T | 2C1)$ to $f(\tau/T | 2C1)$

Within Region 2C1, the pwm ratio defined by equation (4) reduces to

$$\tau/T = (M_1 + M_2 - 1 + 2\epsilon_\tau) / (N_1 + N_2 - 1 + 2\epsilon_T) . \qquad (6)$$

The left-hand-side of Fig. 2 displays the space of $(\epsilon_\tau, \epsilon_T)$ possibilities in 2C1 transformed into $(\epsilon_\tau, \tau/T)$ possibilities by this equation. The boundary equations of T(2C1), are displayed in the Figure by the expressions for ϵ_τ in terms of τ/T. These derive from firstly replacing ϵ_T in (6) by its expression in terms of ϵ_τ on the boundaries of 2C1 on the right-hand-side of Fig. 2: $\epsilon_T = \epsilon_\tau/2$, and $\epsilon_T = \epsilon_\tau$; and from secondly solving the result for ϵ_τ in terms of τ/T. The diagonal line dividing T(2C1) on the left-hand-side of Fig. 2 into two pieces is specified by replacing ϵ_T in equation (6) by 1/2, which is the place at which the algebraic formulation of $f(\epsilon_\tau, \epsilon_T | 2C1)$ changes, as noted in equation (5).

Inverting equation (6) to express ϵ_T in terms of ϵ_τ and τ/T yields

$$\epsilon_T = \frac{M_1 + M_2 - 1 + 2\epsilon_\tau}{2(\tau/T)} - \frac{N_1 + N_2 - 1}{2} \qquad (7)$$

Thus, the density $f(\epsilon_\tau, \epsilon_T | 2C1)$ transforms to $f(\tau/T, \epsilon_\tau | 2C1)$ by replacing ϵ_T in equation (5) by its representation in (6), and multiplying by the Jacobian of the transformation (7), which equals

$$|J| = \frac{(M_1 + M_2 - 1 + 2\epsilon_\tau)}{2(\tau/T)^2} . \qquad (8)$$

In deriving (8) from equation (7), notice that ϵ_T is a *decreasing* function of τ/T, and thus the Jacobian equals the *negative* of the partial derivative of ϵ_T with respect to τ/T.

The final step in deriving the density $f(\tau/T | 2C1)$ is to integrate the joint density $f(\tau/T, \epsilon_\tau | 2C1)$ with respect to ϵ_τ over the relevant domain. Boundary limits on the integration, which must be specified distinctly over three parts of the domain of τ/T, can now be identified simply from the left-hand-side of Fig. 2. To begin, the delimiters of the three zones of integration are identified by replacing the values for the pair $(\epsilon_T, \epsilon_\tau)$ in equation (6) with their values at the four points constituting the vertices of subregions 2C11 and 2C12. These are $(\epsilon_T, \epsilon_\tau) = (0, 0), (1/2, 1/2), (1/2, 1)$, and $(1, 1)$, which yield the four values of τ/T denoted on the left-side axis of Fig. 2. (In viewing the Figure, be

aware that the values of τ/T increase from right to left!) It should be evident from the Figure, then, that

for $\tau/T \in [(M_1+M_2-1)/(N_1+N_2-1),\ (M_1+M_2)/(N_1+N_2)]$,

$$f(\tau/T \mid 2C1) = \int_{[M_1+M_2-1+(N_1+N_2-1)\tau/T]/[\tau/T-2]}^{[M_1+M_2-1+(N_1+N_2-1)\tau/T]/[2\tau/T-2]} f_{2C11}(\tau/T, \epsilon_\tau \mid 2C1)\, d\epsilon_\tau ;$$

for $\tau/T \in [(M_1+M_2)/(N_1+N_2),\ (M_1+M_2+1)/(N_1+N_2+1)]$,

$$f(\tau/T \mid 2C1) = \int_{[M_1+M_2-1+(N_1+N_2-1)\tau/T]/[\tau/T-2]}^{[(N_1+N_2-1)\tau/T-M_1-M_2+1]/2} f_{2C11}(\tau/T, \epsilon_\tau \mid 2C1)\, d\epsilon_\tau ;$$

$$+ \int_{[(N_1+N_2-1)\tau/T-M_1-M_2+1]/2}^{[M_1+M_2-1+(N_1+N_2-1)\tau/T]/[2\tau/T-2]} f_{2C12}(\tau/T, \epsilon_\tau \mid 2C1)\, d\epsilon_\tau ;$$

and for $\tau/T \in [(M_1+M_2+1)/(N_1+N_2+1),\ (M_1+M_2+1)/(N_1+N_2)]$,

$$f(\tau/T \mid 2C1) = \int_{[M_1+M_2-1+(N_1+N_2-1)\tau/T]/[\tau/T-2]}^{[(N_1+N_2-1)\tau/T-M_1-M_2+1]/2} f_{2C11}(\tau/T, \epsilon_\tau \mid 2C1)\, d\epsilon_\tau ;$$

$$+ \int_{[(N_1+N_2-1)\tau/T-M_1-M_2+1]/2}^{1} f_{2C12}(\tau/T, \epsilon_\tau \mid 2C1)\, d\epsilon_\tau ,$$

where the functions denoted by $f_{2C11}(\tau/T, \epsilon_\tau \mid 2C1)$ and $f_{2C12}(\tau/T, \epsilon_\tau \mid 2C1)$ are the two different algebraic forms of the conditional density $f(\tau/T, \epsilon_\tau \mid 2C1)$ we have derived corresponding to smaller and larger values of ϵ_T, respectively. All of this integration is achieved using MAPLE software, and results in a rational function of τ/T which is differentiable over its entire domain, but which has discontinuities in its second derivative at the nodal points where the algebraic form of the density function changes.

To conclude this Section, let us merely notice that the function we have derived as $f(\tau/T, \epsilon_\tau \mid 2C1)$ is identical to the density that would be identified precisely by the denotation

$$f(\tau/T, \epsilon_\tau \mid M_1 < M_2,\ N_1 < N_2,\ \text{and } (\epsilon_0, \epsilon_\tau, \epsilon_T) \in 2C1)$$

For, to repeat our prior assertion under conditions of precise measurement which we extended at the beginning of Section 4, the epsilon vector is assessed as uniform over Region 2C1 when conditioned on Region 2C1 and any observation vector that supports this region as a possibility.

4.3. Pursuing the Parallel Analysis over Region 1C1

We had noted in Table 2 that when $M_1 < M_2$ and $N_1 < N_2$, the only two possible unit-cube-partitioning regions in which the epsilon vector $(\epsilon_0, \epsilon_\tau, \epsilon_T)$ can possibly reside are Regions 1C1 and 2C1. To completely derive the posterior density $f(\tau/T \mid M_1 < M_2 \text{ and } N_1 < N_2)$ we need to pursue next an analysis conditioning on Region 1C1 which exactly mimics in stucture what we have just completed for Region 2C1 in Sections 4.1 and 4.2. Without grinding through all the detail, let us only note that the resulting conditional density is rather different, even to the extent that $f(\tau/T \mid M_1 < M_2,\ N_1 < N_2, \text{ and } (\epsilon_0, \epsilon_\tau, \epsilon_T) \in 1C1)$ is positive over an interval that only overlaps the domain of support for $f(\tau/T \mid 2C1)$, having Heavisdie nodal distinctions at $(M_1+M_2-1)/(N_1+N_2+1)$, $(M_1+M_2-1)/(N_1+N_2-1)$, $(M_1+M_2)/(N_1+N_2)$, and $(M_1+M_2+1)/(N_1+N_2+1)$. Moreover, the probability of Region 1C1 is 1/12, which is twice the probability asserted for Region 2C1.

For a visual summary of the differences between the two conditioning regions, Figs. 3a-3c and Figs. 4a-4c display the distribution function, the density function, and the derivative density function for τ/T given Region 1C1 and 2C1, respectively. Notice the difference in the domains of positive suport and the non-symmetry of the two densities, and the difference of the derivative density function from the almost constant jolt form of the posterior based on a single pulse count, displayed and discussed in Lad and Dunlop (1996).

5. Conglomerating the Conditional Densities over both Regions

The derivations conditioned on the distinct regions being completed, the theorem on total probability allows that the desired conditional density $f(\tau/T \mid M_1 < M_2,\ N_1 < N_2)$ is the marginal probability weighted mixture density

$$(2/3)\, f(\tau/T \mid M_1 < M_2,\ N_1 < N_2, \text{ and } 1C1) + (1/3)\, f(\tau/T \mid M_1 < M_2,\ N_1 < N_2, \text{ and } 2C1).$$

The weights represent $P(1C1 \mid M_1 < M_2,\ N_1 < N_2)$ and $P(2C1 \mid M_1 < M_2,\ N_1 < N_2)$, respectively. Figures 5a-c displays the resulting conglomeration, under the condition of observing $M_1 = 100$, $N_1 = 1000$, $M_2 = 101$, and $N_2 = 1001$. Figures

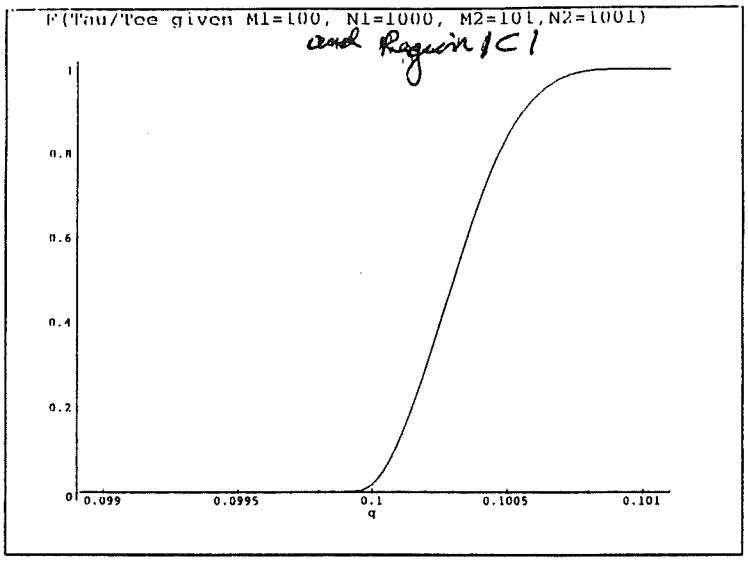

Fig 3a

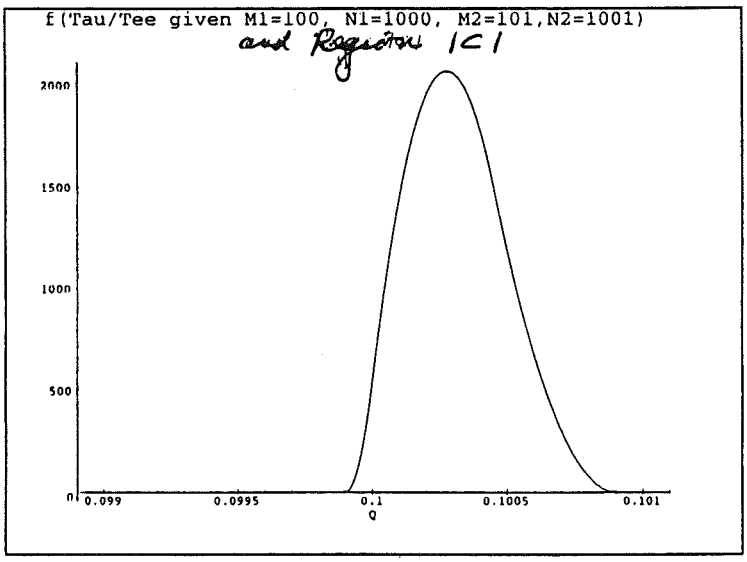

Fig 3b

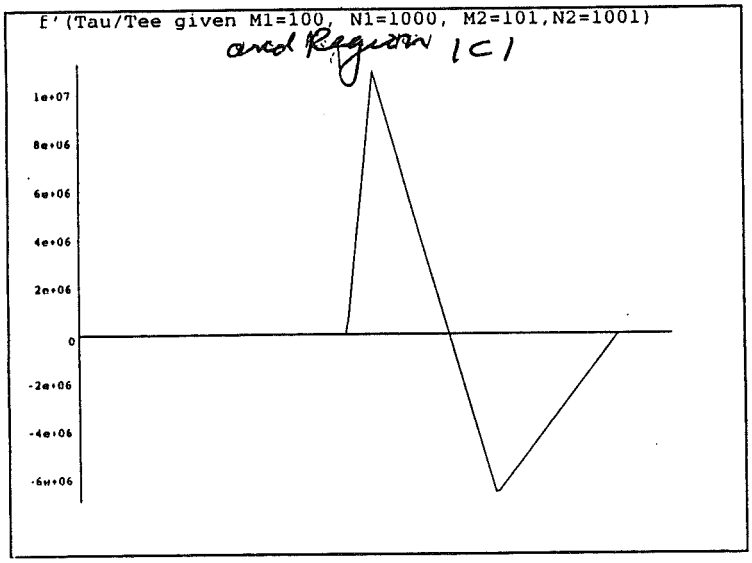

Fig 3c

Lad/Dunlop

p. 12a

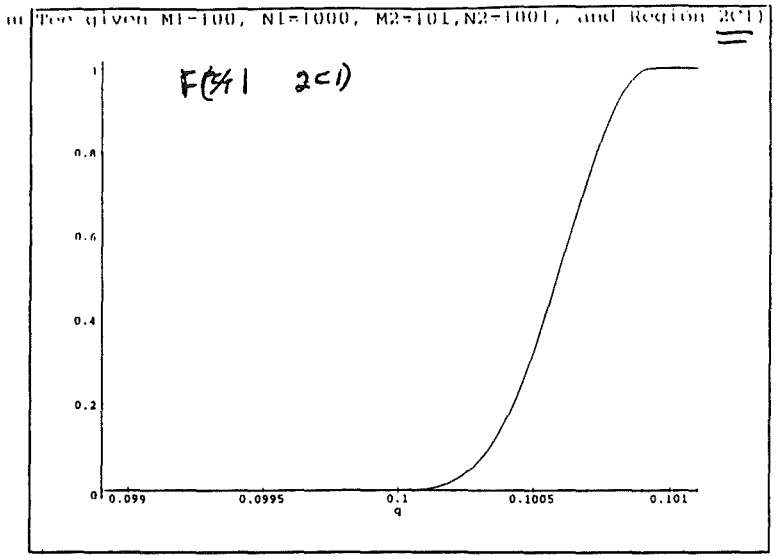

Fig 4a

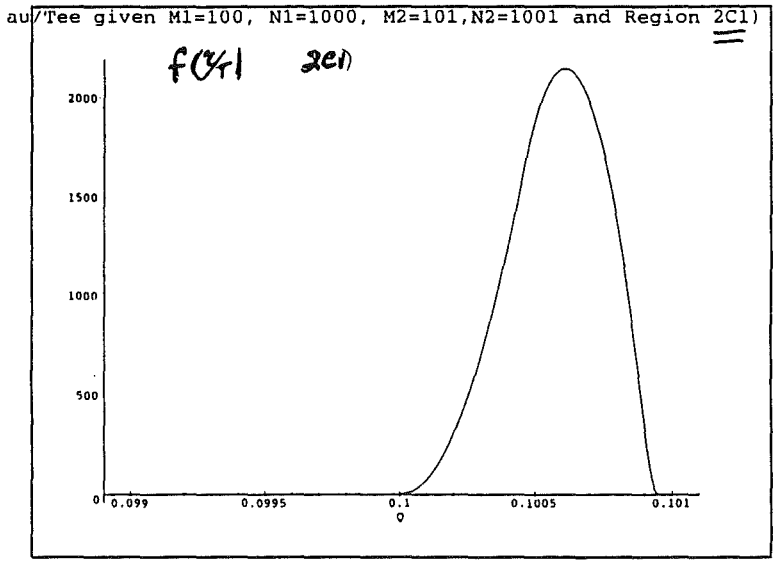

Fig 4b

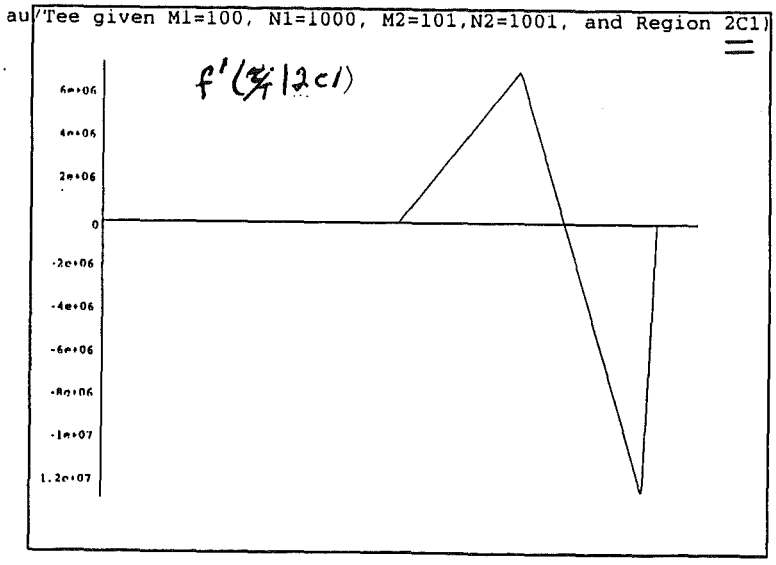

Fig 4c

Sad/Dunlop
p 12 b

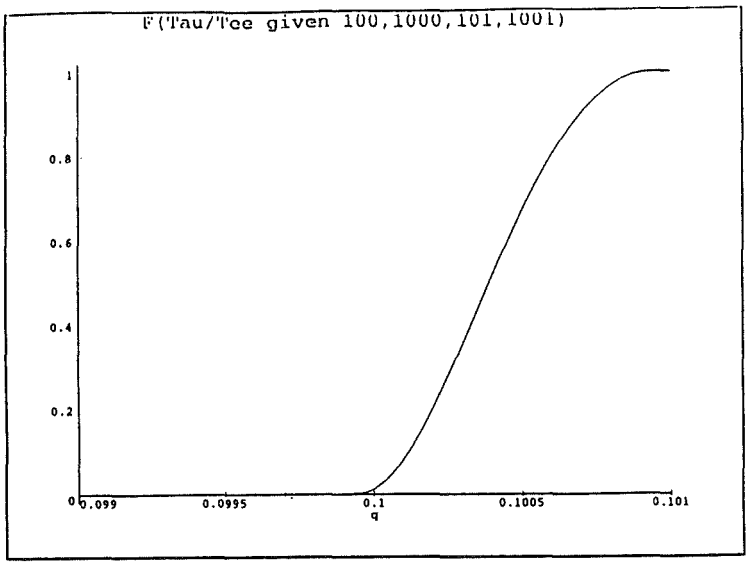

Fig 5a

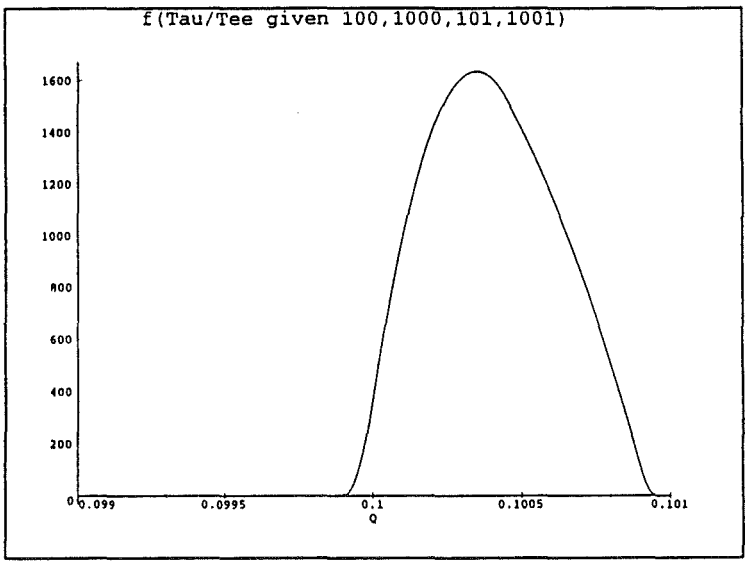

Fig 5b

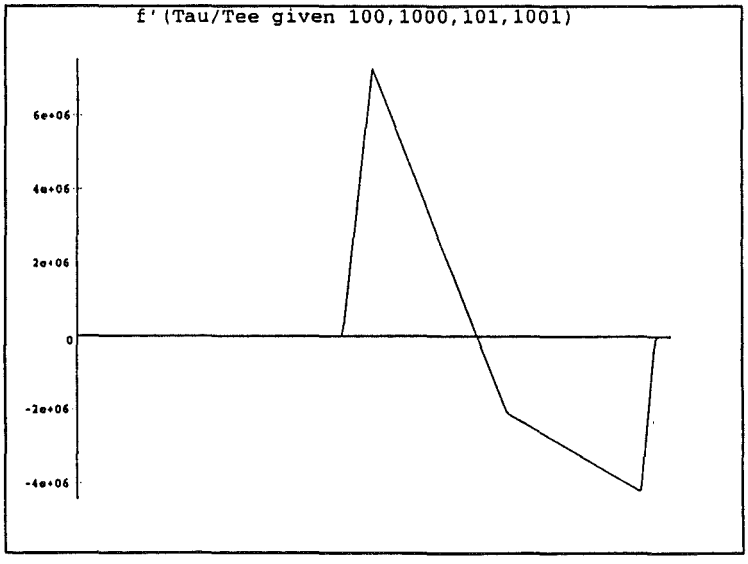

Fig 5c

Ladd / Dunlop
p. 12c

6a-c display the conditional distribution and density given the single pulse observation of $M_1 = 201$ and $N_1 = 2001$, for comparative purposes.

An interesting comparison also results from the summary statistics of the mean and the variance of these two distributions, and also of the posterior distribution when conditioned on only the counts from the first pulse:

$E(\tau/T \mid M_1 = 100, N_1 = 1000) = .0999999333333066$

$V(\tau/T \mid M_1 = 100, N_1 = 1000) = .1516667442222779\ (-6)$

$E(\tau/T \mid M_1 = 201, N_1 = 2001) = .1004497584811512$

$V(\tau/T \mid M_1 = 201, N_1 = 2001) = .3786381415039591\ (-7)$ SD = .1945 (-3)

$E(\tau/T \mid M_1 = 100, N_1 = 1000, M_2 = 101, N_2 = 1001) = .1003997585$

$V(\tau/T \mid M_1 = 100, N_1 = 1000, M_2 = 101, N_2 = 1001) = .4618387734\ (-7)$

SD = .2149 (-3)

So the posterior variance based on these particular counts from two pulses is only slightly larger than the variance conditioned on the single pulse counts from a crystal that vibrates twice as fast! Computing the conditional moments given the two pulse measurements, by the way, requires the use of the well-known formulas for conglomerating moments conditioned on the individual regions: $E(\tau/T) = E_{\text{Regions}}[E(\tau/T \mid \text{Region R})]$, and

$$V(\tau/T) = E_{\text{Regions}}[V(\tau/T \mid \text{Region R})] + V_{\text{Regions}}[E(\tau/T \mid \text{Region R})].$$

6. Concluding Remarks and Further Directions

While the conditional density we have analysed is the simplest among the possible types of conditioning data, it is still quite complicated in its detail. Examing Table 2, the reader can well imagine the intrigue involved in computing the posterior conditioned on $M_1 = M_2$ and $N_1 = N_2$, for example. The density too would be more complicated, exhibiting several more nodal points of changing representation. The results of all such possible conditioning structures will be reported in our promised technical monograph. Some of these will merit intrinsic interest, even though the structure of the logic generating them will be no different than what we have exhibited here. One feature the reader may have noticed, is that the conditional density we have derived here,

$$f(\tau/T \mid M_1 = 100, N_1 = 1000, M_2 = 101, \text{ and } N_2 = 1001),$$

is distinctly different from an alternative

$$f(\tau/T \mid M_1 = 101, N_1 = 1000, M_2 = 100, \text{ and } N_2 = 1001),$$

whose conditioning structure differs only in the order in which the on-state counts of 100 and 101 are recorded for the first and second pulse.

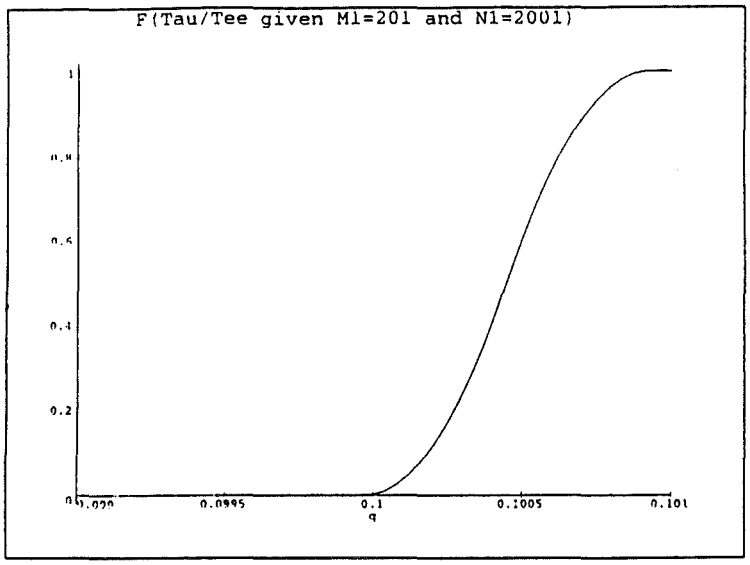

Fig 6a

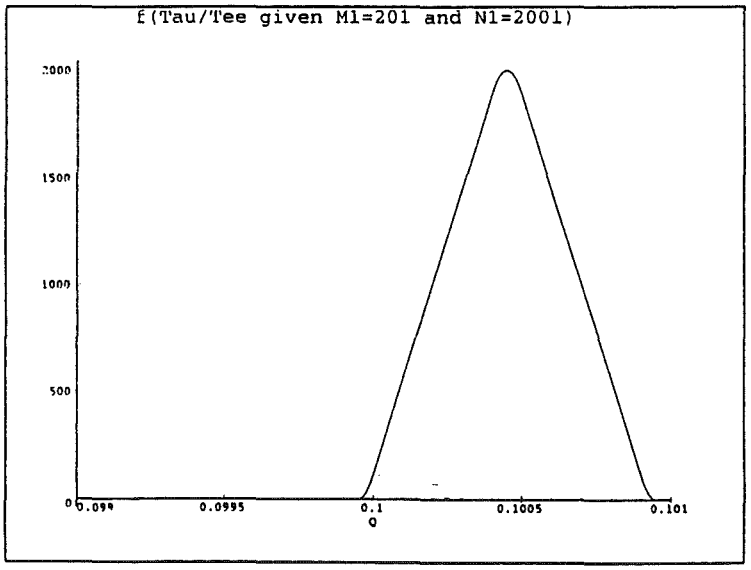

Fig 6b

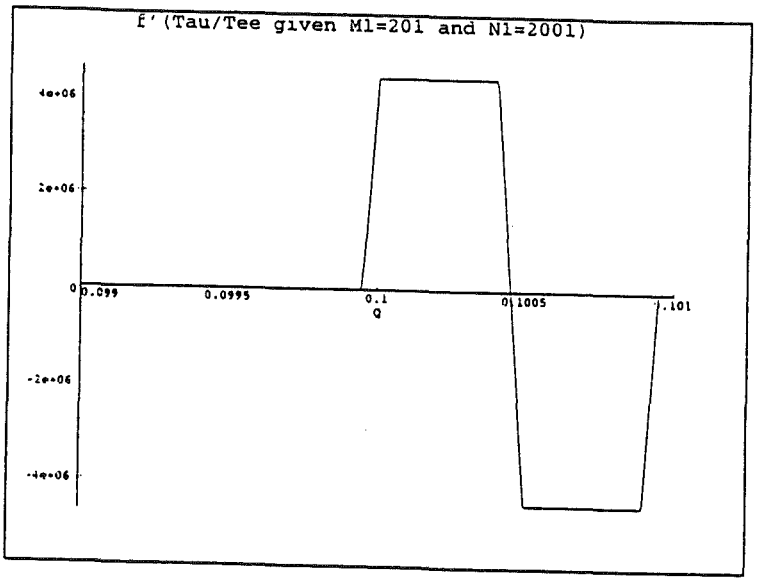

Fig 6c

Sad / Dunlop

p. 13a

Having completed the analysis of the two and multi-pulse count conditioning in the case of exactly repeating signal waves, it is worth concluding by raising the issue of how to analyse the problem when the second signal pulse square wave actually differs from the first. As an extreme case, it is well possible for this to have occurred even when the pulse counts are identical, $M_1 = M_2$ and $N_1 = N_2$. This would be quite an extreme case because of the very short time duration of each wave pulse. We are left then to imagine how the analysis would proceed. Clearly, some prior information regarding the susceptibility of the system signal to change will need to be introduced into the problem. That done, the analsysis would conceivably derive the information conveyed in a string of squarewave signals about the rate of change of the signalling system. For now, we leave that for another day!

Acknowledgement

Thanks to a University of Canterbury research grant for compuational support.

Reference

Lad, F. R. and Dunlop, G. R. (1996) Posterior distribution for the pulse width modulation of a square wave conditional on digital measurements of its on-off components, University of Canterbury Department of Mathematics and Statistics Research Report #134.

Table 1. Partitioning Regions of the Unit-Cube and their Defining Characteristics

Region	Definition	Numerator τ	Denominator T	M_1	N_1	M_2	N_2
1A1	$\epsilon_0 \le \epsilon_1 < \epsilon_\tau < \epsilon_T$	$M_1 + M_2 - 2 + 2\epsilon_\tau$	$N_1 + N_2 - 2 + 2\epsilon_T$	M+1	N+1	M+1	N+1
1A2	$\epsilon_0 < \epsilon_\tau \le \epsilon_1 < \epsilon_T$	$M_1 + M_2 - 1 + 2\epsilon_\tau$	$N_1 + N_2 - 2 + 2\epsilon_T$	M+1	N+1	M	N+1
1A3	$\epsilon_0 < \epsilon_\tau < \epsilon_T \le \epsilon_1$	$M_1 + M_2 - 1 + 2\epsilon_\tau$	$N_1 + N_2 - 1 + 2\epsilon_T$	M+1	N+1	M	N
1B1	$\epsilon_\tau \le \epsilon_0 \le \epsilon_1 < \epsilon_T$	$M_1 + M_2 + 2\epsilon_\tau$	$N_1 + N_2 - 2 + 2\epsilon_T$	M	N+1	M	N+1
1B2	$\epsilon_\tau \le \epsilon_0 < \epsilon_T \le \epsilon_1$	$M_1 + M_2 + 2\epsilon_\tau$	$N_1 + N_2 - 1 + 2\epsilon_T$	M	N+1	M	N
1C1	$\epsilon_1 < \epsilon_\tau < \epsilon_T \le \epsilon_0$	$M_1 + M_2 - 1 + 2\epsilon_\tau$	$N_1 + N_2 - 1 + 2\epsilon_T$	M	N	M+1	N+1
1C2	$\epsilon_\tau \le \epsilon_1 < \epsilon_T \le \epsilon_0$	$M_1 + M_2 + 2\epsilon_\tau$	$N_1 + N_2 - 1 + 2\epsilon_T$	M	N	M	N+1
1C3	$\epsilon_\tau < \epsilon_T \le \epsilon_1 \le \epsilon_0$	$M_1 + M_2 + 2\epsilon_\tau$	$N_1 + N_2 + 2\epsilon_T$	M	N	M	N
2A1	$\epsilon_0 \le \epsilon_1 < \epsilon_T \le \epsilon_\tau$	$M_1 + M_2 - 2 + 2\epsilon_\tau$	$N_1 + N_2 - 2 + 2\epsilon_T$	M+1	N+1	M+1	N+1
2A2	$\epsilon_0 < \epsilon_T \le \epsilon_1 < \epsilon_\tau$	$M_1 + M_2 - 2 + 2\epsilon_\tau$	$N_1 + N_2 - 1 + 2\epsilon_T$	M+1	N+1	M+1	N
2A3	$\epsilon_0 < \epsilon_T \le \epsilon_\tau \le \epsilon_1$	$M_1 + M_2 - 1 + 2\epsilon_\tau$	$N_1 + N_2 - 1 + 2\epsilon_T$	M+1	N+1	M	N
2B1	$\epsilon_1 < \epsilon_T \le \epsilon_0 < \epsilon_\tau$	$M_1 + M_2 - 2 + 2\epsilon_\tau$	$N_1 + N_2 - 1 + 2\epsilon_T$	M+1	N	M+1	N+1
2B2	$\epsilon_T \le \epsilon_1 \le \epsilon_0 < \epsilon_\tau$	$M_1 + M_2 - 2 + 2\epsilon_\tau$	$N_1 + N_2 + 2\epsilon_T$	M+1	N	M+1	N
2C1	$\epsilon_1 < \epsilon_T \le \epsilon_\tau \le \epsilon_0$	$M_1 + M_2 - 1 + 2\epsilon_\tau$	$N_1 + N_2 - 1 + 2\epsilon_T$	M	N	M+1	N+1
2C2	$\epsilon_T \le \epsilon_1 < \epsilon_\tau \le \epsilon_0$	$M_1 + M_2 - 1 + 2\epsilon_\tau$	$N_1 + N_2 + 2\epsilon_T$	M	N	M+1	N
2C3	$\epsilon_T \le \epsilon_\tau \le \epsilon_1 \le \epsilon_0$	$M_1 + M_2 + 2\epsilon_\tau$	$N_1 + N_2 + 2\epsilon_T$	M	N	M	N

Paul / Dunlop
p. 14a

Table 2. Relational Patterns of Vibration Counts M_1, N_1, M_2, and N_2 within Regions

Relation		Region	Probability	Exact Condition			
$M_1 < M_2$	$N_1 < N_2$	1C1	1/12	$M_1 = M$	$N_1 = N$	$M_2 = M+1$	$N_2 = N+1$
		2C1	1/24	$M_1 = M$	$N_1 = N$	$M_2 = M+1$	$N_2 = N+1$
$M_1 < M_2$	$N_1 = N_2$	2C2	1/24	$M_1 = M$	$N_1 = N$	$M_2 = M+1$	$N_2 = N$
$M_1 < M_2$	$N_1 > N_2$	Impossible					
$M_1 = M_2$	$N_1 < N_2$	1C2	1/24	$M_1 = M$	$N_1 = N$	$M_2 = M$	$N_2 = N+1$
		2B1	1/12	$M_1 = M+1$	$N_1 = N$	$M_2 = M+1$	$N_2 = N+1$
$M_1 = M_2$	$N_1 = N_2$	1A1	1/12	$M_1 = M+1$	$N_1 = N+1$	$M_2 = M+1$	$N_2 = N+1$
		1B1	1/12	$M_1 = M$	$N_1 = N+1$	$M_2 = M$	$N_2 = N+1$
		1C3	1/24	$M_1 = M$	$N_1 = N$	$M_2 = M$	$N_2 = N$
		2A1	1/24	$M_1 = M+1$	$N_1 = N+1$	$M_2 = M+1$	$N_2 = N+1$
		2B2	1/12	$M_1 = M+1$	$N_1 = N$	$M_2 = M+1$	$N_2 = N$
		2C3	1/12	$M_1 = M$	$N_1 = N$	$M_2 = M$	$N_2 = N$
$M_1 = M_2$	$N_1 > N_2$	1B2	1/12	$M_1 = M$	$N_1 = N+1$	$M_2 = M$	$N_2 = N$
		2A2	1/24	$M_1 = M+1$	$N_1 = N+1$	$M_2 = M+1$	$N_2 = N$
$M_1 > M_2$	$N_1 < N_2$	Impossible					
$M_1 > M_2$	$N_1 = N_2$	1A2	1/24	$M_1 = M+1$	$N_1 = N+1$	$M_2 = M$	$N_2 = N+1$
$M_1 > M_2$	$N_1 > N_2$	1A3	1/24	$M_1 = M+1$	$N_1 = N+1$	$M_2 = M$	$N_2 = N$
		2A3	1/12	$M_1 = M+1$	$N_1 = N+1$	$M_2 = M$	$N_2 = N$

Fad / Dunlop
p. 14 b